Published OnlineFirst January 31, 2019; DOI: 10.1158/1078-0432.CCR-18-3684

Translational Cancer Mechanisms and Therapy

Clinical Cancer Research

Loss of SMAD4 Promotes Colorectal Cancer Progression by Recruiting Tumor-Associated Neutrophils via the CXCL1/8–CXCR2 Axis

Ryotaro Ogawa[1], Takamasa Yamamoto[1], Hideyo Hirai[2], Keita Hanada[1], Yoshiyuki Kiyasu[1], Gen Nishikawa[1], Rei Mizuno[1], Susumu Inamoto[1], Yoshiro Itatani[1], Yoshiharu Sakai[1], and Kenji Kawada[1]

Abstract

Purpose: SMAD4 is a key transcriptional factor of TGFβ signaling and acts as a tumor suppressor in colorectal cancer. In the present study, we explored the immunologic effect of SMAD4 on the tumor microenvironment.

Experimental Design: Using 99 clinical specimens and human colorectal cancer cell lines, we investigate the relationship between SMAD4 expression and neutrophil accumulation. We immunohistochemically analyzed expression of SMAD4, CXCL1, CXCL8, CXCR2, and other proteins with clinical specimens. Finally, we determined the serum levels of CXCL1 and CXCL8 in 125 patients with colorectal cancer.

Results: SMAD4 knockdown from human colorectal cancer cells upregulated the expression of CXCL1 and CXCL8, which recruited neutrophils to colorectal cancer tumor via CXCR2. In turn, when neutrophils were exposed to the supernatant of SMAD4-negative colorectal cancer cells, they produced a large amount of CXCL1 and CXCL8 by themselves *in vitro*. In human clinical specimens, we found that neutrophil infiltration into the peritumoral stroma was more marked in SMAD4-negative colorectal cancer compared with that in SMAD4-positive colorectal cancer, and that both CXCL1 and CXCL8 were abundantly expressed in the tumor-infiltrating neutrophils. Neutrophils isolated from primary colorectal cancer expressed significantly higher levels of CXCL1 and CXCL8 than did those isolated from peripheral blood. Furthermore, tumor-infiltrating neutrophils expressed MMP2 and MMP9 in addition to ARG1 and IDO. Serum CXCL8 level was significantly higher in colorectal cancer patients, especially those at stage II/III, and statistical analysis indicated a high CXCL8 level was associated with a shorter overall survival and relapse-free survival.

Conclusions: Blockade of the CXCL1/8–CXCR2 axis could be a novel therapeutic approach against SMAD4-negative colorectal cancer.

Introduction

Colorectal cancer is the third most common cause of cancer-related deaths worldwide. Colorectal cancer is thought to result from the accumulation of genetic alterations such as oncogenes and tumor suppressor genes (e.g., *APC*, *Kras*, *p53*, and *SMAD4*) as well as epigenetic changes of additional genes. SMAD4 is a downstream mediator of the transforming growth factor-β (TGFβ) signaling superfamily and acts as a tumor suppressor in colorectal cancer. Loss of the SMAD4 protein is observed in 30% to 40% of colorectal cancer cases and is associated with a poor prognosis (1, 2). In mouse models, inactivation of the *Smad4* gene in the intestinal epithelium in the context of *Apc* mutation resulted in the formation of invasive adenocarcinoma with a prominent accumulation of bone marrow–derived myeloid cells via the CCL9–CCR1 axis (3, 4). Using human colorectal cancer samples, we previously found that loss of SMAD4 in human colorectal cancer cells resulted in the upregulation of CCL15 (the human orthologue of mouse CCL9), which caused the recruitment of $CCR1^+$ myeloid cells via the CCL15–CCR1 axis to facilitate tumor invasion and metastasis (5–7). We observed that most $CCR1^+$ cells recruited to the primary colorectal cancer and metastatic colorectal cancer were myeloid-derived suppressor cell (MDSC) and neutrophil phenotypes, respectively (5–7). In a recent publication, Means and colleagues reported that SMAD4 loss in colonic epithelium activated inflammatory cell infiltration and promoted tumor progression through regulating a number of chemokines and cytokines (8).

Tumor–stromal interaction in the tumor microenvironment is implicated in tumor progression. Clinical relevance of immune cell infiltration in colorectal cancer tissues has been investigated. Although infiltration of $CD3^+$ T cells and cytotoxic $CD8^+$ T cells has been associated with a favorable prognosis (9), the value of the innate myeloid cells is unclear. Emerging evidence has indicated that various types of myeloid cells, such as macrophages and neutrophils, play important roles in tumor progression, that is, as tumor-associated macrophages (TAM) and tumor-associated neutrophils (TAN; refs. 10–12). Neutrophils account for 50% to

[1]Department of Surgery, Graduate School of Medicine, Kyoto University, Kyoto, Japan. [2]Department of Transfusion Medicine and Cell Therapy, Graduate School of Medicine, Kyoto University, Kyoto, Japan.

Note: Supplementary data for this article are available at Clinical Cancer Research Online (http://clincancerres.aacrjournals.org/).

R. Ogawa and T. Yamamoto contributed equally to this article.

Corresponding Author: Kenji Kawada, Graduate School of Medicine, Kyoto University, 54 Shogoin-Kawara-cho, Sakyo-ku, Kyoto 606-8507, Japan. Phone: 81-75-366-7595; Fax: 81-75-366-7642; E-mail: kkawada@kuhp.kyoto-u.ac.jp

doi: 10.1158/1078-0432.CCR-18-3684

©2019 American Association for Cancer Research.

Downloaded from clincancerres.aacrjournals.org on June 30, 2019. © 2019 American Association for Cancer Research.

Published OnlineFirst January 31, 2019; DOI: 10.1158/1078-0432.CCR-18-3684

Translational Relevance

Although the infiltration of $CD3^+$ T cells and cytotoxic $CD8^+$ T cells into colorectal cancer tissues has been associated with a favorable prognosis, the value of the innate myeloid cells is unclear. Various types of myeloid cells, such as macrophages and neutrophils, play important roles in tumor progression. Clinical significance of neutrophil-infiltrating colorectal cancer is unclear, and underlying functional mechanisms remains to be elucidated. This is the first clinical study showing that loss of SMAD4 from colorectal cancer cells resulted in the secretion of CXCL1 and CXCL8 to recruit $CXCR2^+$ neutrophils, and that, in turn, the recruited neutrophils abundantly produced CXCL1 and CXCL8, which could help to further accumulate $CXCR2^+$ neutrophils and result in an amplification of the cytokine/chemokine milieu shaped by the CXCL1/8–CXCR2 axis. Serum CXCL8 levels in patients with colorectal cancer were associated with patients' prognosis. These results suggest that blockade of the CXCL1/8–CXCR2 axis could be a novel therapeutic approach against SMAD4-negative colorectal cancer.

70% of all leukocytes in humans and have been recognized as a first-line host defender against infectious pathogens. In addition to direct bactericidal activities, neutrophils regulate angiogenesis and tissue regeneration against tissue damage by release of multiple proteases. A number of studies have shown that high levels of circulating neutrophils and neutrophil-to-lymphocyte ratio in peripheral blood are associated with poor prognosis in several types of cancer, which emphasizes the importance of neutrophils in cancer biology (13). The role of neutrophils in the tumor microenvironment and the clinical significance of neutrophil infiltration into cancer tissues are controversial (11, 14). Recent studies have suggested that local microenvironmental conditions might result in the polarization of neutrophils toward a pro- or antitumor state (15, 16). Clinical significance of TAN-infiltrating colorectal cancer is unclear, and underlying functional mechanisms remain to be elucidated.

Here, we report that loss of SMAD4 from human colorectal cancer cells resulted in a significant increase of CXCL1 and CXCL8 expression, which was associated with the recruitment of neutrophils via CXCR2. In turn, when neutrophils were exposed to the supernatant of SMAD4-negative colorectal cancer cells, they produced a large amount of CXCL1 and CXCL8 *in vitro*. In human clinical specimens, we found that the density of neutrophils around the peritumoral stroma was higher in SMAD4-negative colorectal cancers than that in SMAD4-positive ones, and that both CXCL1 and CXCL8 were abundantly expressed in the tumor-infiltrating neutrophils. We further showed that the neutrophils isolated from primary colorectal cancer expressed significantly higher levels of CXCL1 and CXCL8 than did those isolated from peripheral blood. Serum CXCL8 level was significantly higher in patients with colorectal cancer, especially those at stage II/III, and statistical analysis indicated that the patients with colorectal cancer with high CXCL8 level exhibited a shorter overall survival (OS) and relapse-free survival (RFS) compared with those with low CXCL8 level. These results suggest that blocking the CXCL1/8–CXCR2 axis may provide the possibility of a novel therapeutic strategy for colorectal cancer, and that serum CXCL8 level could be a predictive biomarker for the prognosis of colorectal cancer patients.

Materials and Methods

Patients' population

A total of 99 patients with colorectal cancer underwent primary resection at Kyoto University Hospital between 2005 and 2006, and their tissue samples were analyzed retrospectively. Serum CXCL1 and CXCL8 levels were measured using preoperative serum samples collected from 125 patients with colorectal cancer and 11 healthy donors between 2011 and 2018. Written informed consent for the use of serum and resected samples was obtained from all patients in accordance with the Declaration of Helsinki, and these study protocols were approved by the Institutional Review Board of Kyoto University.

Cell lines and reagents

SW837, SW480, Caco2, and HT29 were obtained from ATCC. The identity of cell line was confirmed by STR analysis (Takara Bio CDM Center). These cells were cultured in low glucose DMEM with 10% fetal bovine serum and 1% penicillin/streptomycin mixture. Stable transductants of HT29 and SW480 cells for cMyc-tagged *SMAD4* were established, as previously described (5–7). Stable transductants of SW837 cells with shRNA against *SMAD4* or scramble shRNA were established, as previously described (5–7). A detailed list of the antibodies and kinase inhibitors used is shown in Supplementary Tables S1 and S2.

IHC and immunofluorescence analysis

Formalin-fixed, paraffin-embedded sections were used for IHC and immunofluorescence analysis. For IHC, tissue sections following antigen retrieval were incubated with respective primary antibodies (Supplementary Table S1) overnight at 4°C, and stained by the avidin–biotin immunoperoxidase method. SMAD4 expression was evaluated as a nuclear staining, and the percentage of positively stained cells was scored, as previously described (7). We quantified the densities of $CD66b^+$ cells around the peritumoral stroma, and the average of 5 to 7 fields (0.1 mm^2) analyzed per 1 sample, as previously described (5–7). Three researchers (R. Ogawa, T. Yamamoto, and K. Kawada) evaluated IHC samples without prior knowledge of other data. The slides with different evaluations among 3 researchers were reinterpreted at a conference to reach the consensus. For immunofluorescence analysis, tissue sections following antigen retrieval were incubated with primary antibodies (Supplementary Table S1) overnight at 4°C and stained with fluorescence-labeled second antibody (Alexa Fluor 488 anti-goat, Alexa Fluor 488 anti-mouse, Alexa Fluor 594 anti-mouse, or Alexa Fluor 594 anti-rabbit). Representative photos were taken using a fluorescence microscope (BZX-710; Keyence).

Western blotting

Cells were lysed in NP40 buffer (50 mmol/L Tris [pH 7.6], 150 mmol/L NaCl, 1% NP40, 10% glycerol) containing protease inhibitor cocktail (Nacalai tesque) and phosphatase inhibitor cocktail (Nacalai tesque). Proteins were separated by using SDS-PAGE gels and transferred to PVDF membranes. After blocking membranes with Blocking One (Nacalai tesque), these were incubated with the primary antibodies, followed by

Downloaded from clincancerres.aacrjournals.org on June 30, 2019. © 2019 American Association for Cancer Research.

Published OnlineFirst January 31, 2019; DOI: 10.1158/1078-0432.CCR-18-3684

HRP-conjugated secondary antibodies. Antibodies list was shown in Supplementary Table S1.

Quantitative reverse transcription polymerase chain reaction (qRT-PCR)

Total RNA was extracted using a High Pure RNA extraction kit (Roche) and RNeasy Micro kit (Qiagen), according to the manufacture's protocol. cDNA synthesized by ReverTra ace qPCR RT kit (Toyobo Co. Ltd.) was quantified using Step One Plus real-time PCR system (Thermo Fisher Scientific Inc.). TaqMan Gene-Expression assays (Thermo Fisher Scientific Inc.) were used for the primers and probes of *CXCL1* (assay ID, Hs00236937_m1), *CXCL8* (Hs00174103_m1), *ATCB* (Hs01060665_g1), and *GAPDH* (Hs02786624_g1). The mRNA levels were normalized to those for *ACTB* or *GAPDH* using the ΔΔCT method.

RNA interference

To knockdown the endogenous SMAD4 expression, 2 distinct siRNA for *SMAD4* (FlexiTube siRNA_SI00076041 and SI03089527) and negative control (FlexiTube siRNA SI03650318) were used from Qiagen. The siRNA (10 nmol/L) was transfected into CaCo2 cells with Lipofectamine RNAiMAX (Thermo Fisher Scientific Inc.). Cells were harvested in 48 to 72 hours.

5′ Rapid amplification cDNA ends (5′ RACE)

5′ RACE analysis of *CXCL1* and *CXCL8* was performed using cDNA from SW837 cells and Gene Racer Kit (Thermo Fisher Scientific Inc.) with reverse CXCL1 gene-specific primer (5′-TCCGGGGGACTTCACGTTCACAC-3′) and reverse CXCL8 gene-specific primer (5′-TGTTGGCGCAGTGTGGTCCACTC-3′) according to the manufacturer's protocol.

Luciferase reporter assay

Cells were transfected with firefly luciferase reporter gene constructs and pGL4.74 vector (Promega), using Lipofectamine LTX (Thermo Fisher Scientific Inc.). The promoter regions of *CXCL1* and *CXCL8* were cloned by PCR amplification from the genomic DNA of SW837 cells. The following primers were used to amplify promoter region: *CXCL1* forward, 5′-CTCGAGGCCCCTGGGG-CAGAAGCCTC-3′; *CXCL1* reverse, 5′-GATATCGGGGCTCAG-CAGGCGGGTCT-3′; *CXCL8* forward, 5′-CTCGAGTTCACAGTGT-GGGCAAATTC-3′; *CXCL8* reverse, 5′-GATATCGTTTACACACA-GTGAGATGG-3′. Each amplified promoter region was inserted into pGL4.10 luciferase vector (Promega). Cells were transfected with these vectors for 18 hours, and then treated for 6 hours with or without 10 ng/mL TGFβ1 (PeproTech). Firefly and Renilla luciferase activities were determined using the Dual-Luciferase Reporter Assay system (Promega) with a GloMax-Multi+ detection system E8032LD (Promega). The activities of firefly luciferase were normalized against those of Renilla.

Chromatin immunoprecipitation-polymerase chain reaction (ChIP-PCR)

The ChIP-PCR was performed using ChIP-IT Express kit (Qiagen) according to the manufacture's protocol. To immunoprecipitate SMAD4 protein, anti-SMAD4 antibody (B-8; Santa Cruz) was used. The DNA fragment that was immunoprecipitated by anti-SMAD4 antibody was analyzed quantitative PCR by using THUNDERBIRD SYBR qPCR mix (Toyobo). The primer sets were described in Supplementary Table S3.

Enzyme-linked immunosorbent assay (ELISA)

Preoperative serum protein levels of CXCL1 and CXCL8 were measured using DuoSet Human ELISA kit for CXCL1 and CXCL8 (R&D Systems), according to the manufacture's protocol.

Chemokine antibody array, angiogenesis antibody array, and phospho-kinase array

After SW837-scramble and SW837-sh*SMAD4* #2 cells were cultured for 24 hours, conditioned media were collected and filtered through filter sterilization. Neutrophils from healthy donor were cultured with the conditioned media. After incubation, neutrophils were collected and lysed in lysis buffer with protease inhibitor cocktail. Human chemokine antibody array (RayBiotech), human angiogenesis antibody array (RayBiotech), and Proteome Profiler Human Phospho-Kinase Array Kit (R&D Systems) were used, according to the manufacture's protocol.

Chemotaxis assay

Neutrophils from healthy donor were isolated using the MACSxpress whole blood neutrophil isolation kit (Miltenyi Biotec), according to the manufacture's protocol. Neutrophil migration was measured in transwell chamber (3 μm; Corning Costar). Neutrophils (1×10^5 cells) were added to the upper chamber, whereas the supernatant of colorectal cancer cells was added to the lower chamber. Neutralizing antibodies for CXCL1 and/or CXCL8 (R&D Systems) were added to the lower chamber. Neutrophils were treated with SB225002 (Tocris Bioscience) before applying to the upper chamber. After 2 hours of incubation, the number of neutrophils located in the lower chamber was counted using ACCURI C6 (BD Biosciences).

Flow cytometry

A total of 6 pairs of fresh colorectal cancer tissues and peripheral blood samples were obtained to isolate neutrophils using FACSAria. In brief, tumor tissues were minced and incubated with tumor dissociation kit (Miltenyi Biotec). To raise the purity of leukocytes, cells were labeled with anti-human biotin-conjugated CD45 antibody (Miltenyi Biotec) and antibiotin microbeads (Miltenyi Biotec). These labeled cells were selected by using magnetic-activated cell sorting columns (Miltenyi Biotec) according to the manufacture's protocol. Subsequently, leukocytes obtained from tissue sample and preoperative blood were labeled with antibodies shown in Supplementary Table S4. Dead cells were stained with PI and gated out. After gating, neutrophils labeled $CD45^+$, $CD66b^+$, $CD15^+$, $CD16^+$, and $CD14^-$ were sorted. To test the purity of neutrophils gained using the MACSxpress neutrophil isolation kit (Miltenyi Biotec), we stained cell suspension with FITC-conjugated anti-CD66b (BioLegend), APC-conjugated anti-CXCR2 (BD Biosciences), and corresponding isotype controls. The samples were analyzed on ACCURI C6. The data analysis was performed using FlowJo software (Tree Star Inc.).

Statistical analysis

All results were confirmed using at least 3 independent *in vitro* experiments, and data from 1 representative experiments were presented. Analyzed values are expressed as means ± standard deviation (SD). Categorical data were determined with the χ^2 test. Continuous variables were determined with Student *t* test or Wilcoxon test. The log-rank test or Wilcoxon test was used for analysis of OS and RFS. All analyses were 2-sided, and

Downloaded from clincancerres.aacrjournals.org on June 30, 2019. © 2019 American Association for Cancer Research.

Published OnlineFirst January 31, 2019; DOI: 10.1158/1078-0432.CCR-18-3684

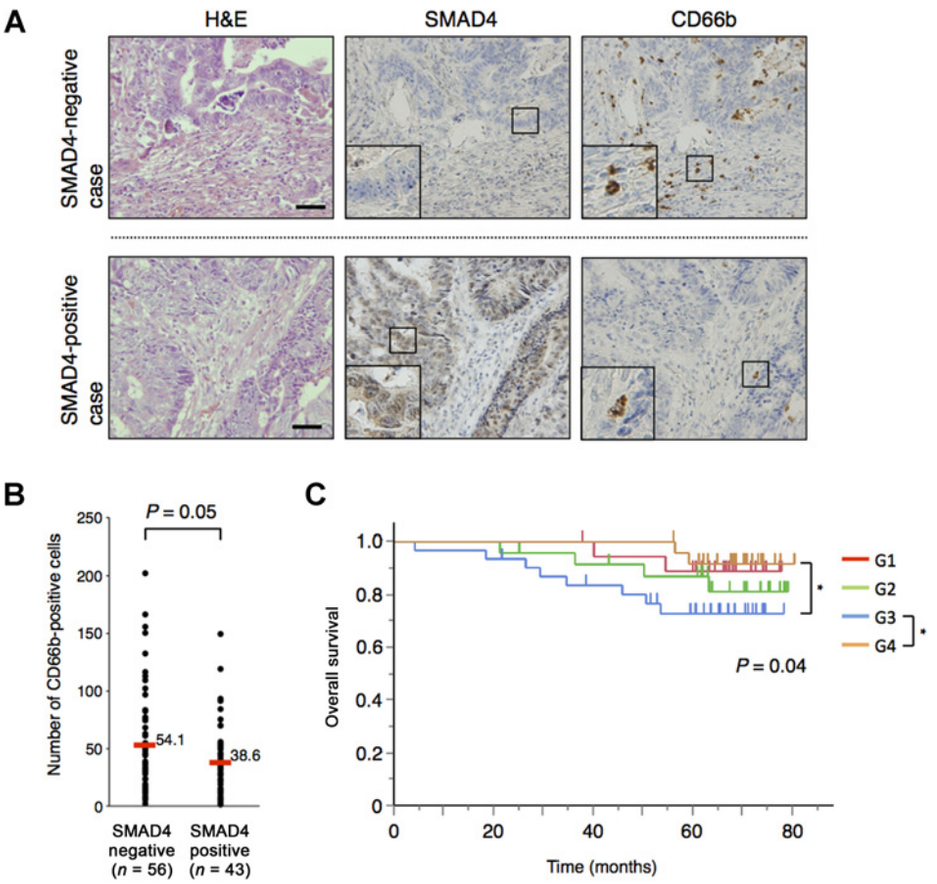

		Number of CD66b-positive cells	
		≥ 35.8	< 35.8
SMAD4	Positive	G1 (n = 19)	G2 (n = 24)
	Negative	G3 (n = 31)	G4 (n = 25)

Figure 1.
Correlation of SMAD4 loss and CD66b$^+$ neutrophil accumulation. **A,** Hematoxylin and eosin staining (H&E) and IHC detection of SMAD4 and CD66b in primary colorectal cancer. Top and bottom, serial sections of representative SMAD4-negative and SMAD4-positive colorectal cancer, respectively. Scale bar, 50 μm. **B,** Quantification of CD66b$^+$ cell density in primary colorectal cancer with and without SMAD4 expression (n = 43 and 56, respectively). Student t test. Horizontal bars show the mean. **C,** Kaplan–Meier plot for OS. Patients with colorectal cancer were divided into 4 groups based on SMAD4 expression and the number of CD66b$^+$ neutrophil infiltration. The median number (i.e., 35.8) was used as cutoff value. *, $P < 0.05$ by Wilcoxon test.

P value with < 0.05 was considered as statistically significant. Statistical analyses were performed using JMP Pro software, version 13.0.0 (SAS Institute Inc.).

Results

Loss of SMAD4 from colorectal cancer cells accumulates CD66b$^+$ neutrophils

We previously reported that loss of SMAD4 from colorectal cancer causes accumulation of CCR1$^+$ myeloid cells via the CCL15–CCR1 chemokine axis to facilitate tumor invasion and metastasis (5–7). Given that myeloid cells express several types of chemokine receptors, we hypothesized that the recruitment of myeloid cells could be taking place in the tumor microenvironment via chemokine receptors other than CCR1. A better understanding of the mechanisms how colorectal cancer recruits myeloid cells to the tumor sites may lead to more effective therapy.

To investigate the relationship between SMAD4 expression and neutrophil accumulation, we examined 99 primary colorectal cancer samples by IHC (Supplementary Table S5). SMAD4 expression was negative in 57% (56/99) and positive in 43% (43/99) of the colorectal cancer samples (Fig. 1A). Cells expressing CD66b, a neutrophil marker, were mainly accumulated around the peritumoral stroma. The number of CD66b$^+$ neutrophils was higher in SMAD4-negative colorectal cancers than that in SMAD4-positive ones (median, 54.1 vs. 38.6, respectively; $P = 0.05$; Fig. 1B).

We next examined the effect of CD66b$^+$ neutrophil infiltration on the prognosis of patients with colorectal cancer. We classified these 99 samples into 4 groups based on SMAD4 expression and the number of CD66b$^+$ neutrophil infiltration. OS was significantly lower in the patients with negative SMAD4 expression and high neutrophil infiltration compared with those with negative SMAD4 expression and low neutrophil infiltration ($P = 0.04$; Fig. 1C).

Expression levels of CXCL1 and CXCL8 are inversely correlated with SMAD4 expression in human colorectal cancer cell lines

In order to elucidate the mechanism how SMAD4 regulates the CD66b$^+$ neutrophil infiltration, we used 4 colorectal cancer cell lines. SW837 and Caco2 express wild-type SMAD4, while SW480 and HT29 lack SMAD4 (Fig. 2A). First, we introduced 2 short hairpin RNA (shRNA) constructs targeting *SMAD4* (referred to as sh*SMAD4* #1 and sh*SMAD4* #2) into SW837 cells, and confirmed that these sh*SMAD4* constructs dramatically decreased

Downloaded from clincancerres.aacrjournals.org on June 30, 2019. © 2019 American Association for Cancer Research.

Published OnlineFirst January 31, 2019; DOI: 10.1158/1078-0432.CCR-18-3684

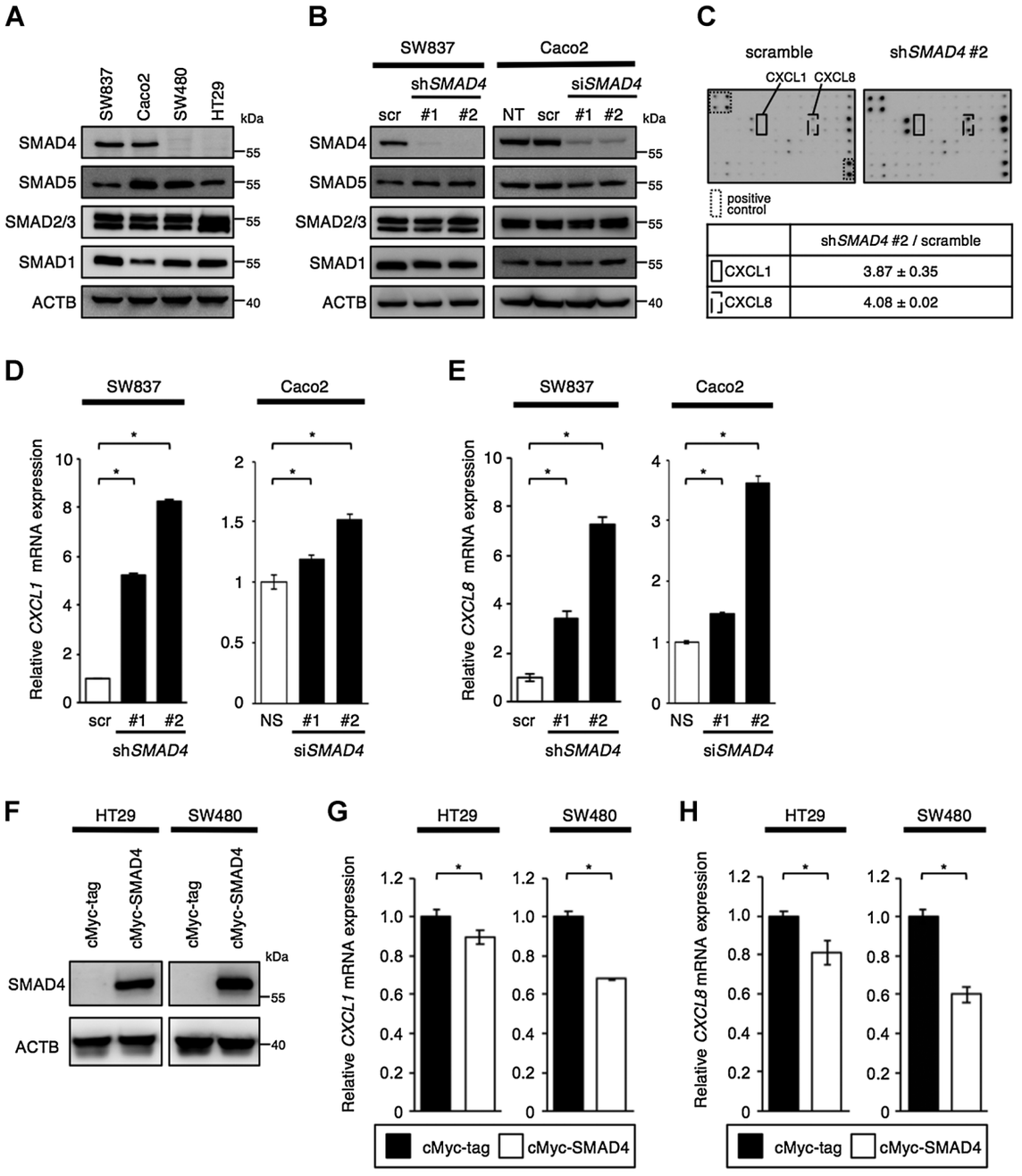

Figure 2.

Relationship between SMAD4 and CXCL1/8 in human colorectal cancer cell lines. **A,** Western blot analysis showing SMAD4, SMAD5, SMAD2/3, SMAD1, and b-actin (ACTB). **B,** Construction of *SMAD4*-knockdown cells by sh*SMAD4* or si*SMAD4*. NT and scr indicate nontreatment and nonsilencing scramble as controls. **C,** Chemokine array using the SW837 cells engineered with stable *SMAD4*-knockdown (SW837-sh*SMAD4* #2) and scramble control. **D** and **E,** qRT-PCR analysis for *CXCL1* (**D**) and *CXCL8* (**E**). *, $P < 0.05$ by Student *t* test. **F,** Construction of stable transductants for cMyc-tagged *SMAD4*. **G** and **H,** qRT-PCR analysis for *CXCL1* (**G**) and *CXCL8* (**H**). *, $P < 0.05$ by Student *t* test.

SMAD4 expression (Fig. 2B, left). We also confirmed that these sh*SMAD4* constructs did not affect the expression of other proteins in the SMAD family. Although we could not establish the stable *SMAD4*-knockdown Caco2 cells, we confirmed that 2 small interfering RNA (siRNA) constructs (si*SMAD4* #1 and si*SMAD4* #2) transiently knocked down SMAD4 expression in Caco2 cells (Fig. 2B, right).

To identify the determinants responsible for neutrophil infiltration, we conducted a chemokine array containing a panel of chemokines using the SW837 cells engineered with stable

Downloaded from clincancerres.aacrjournals.org on June 30, 2019. © 2019 American Association for Cancer Research.

Published OnlineFirst January 31, 2019; DOI: 10.1158/1078-0432.CCR-18-3684

SMAD4-knockdown (SW837-sh*SMAD4* #2). Of note, the secretion of a subset of chemokines was elevated in SW837-sh*SMAD4* cells compared with that in SW837-scramble control cells (Supplementary Fig. S1A), and the most upregulated chemokines by SMAD4 loss were CXCL1 and CXCL8 (Fig. 2C). We also confirmed that *CXCL1* and *CXCL8* were significantly elevated in SW837 and Caco2 cells when *SMAD4* was knocked down, as determined by quantitative reverse transcription polymerase chain reaction (qRT-PCR; Fig. 2D and E). To validate that the levels of CXCL1 and CXCL8 were affected by SMAD4, we next investigated whether exogenous expression of SMAD4 could affect CXCL1 and CXCL8 expression in SMAD4-deficient cell lines (HT29 and SW480). When cMyc-tagged SMAD4 was stably expressed in HT29 and SW480 cells by lentiviral transfection (Fig. 2F), the mRNA levels of *CXCL1* and *CXCL8* were significantly decreased compared with those of the control cells (Fig. 2G and H). We also found that TGFβ1 stimulation led to further reduction of CXCL1 and CXCL8 (data not shown). These results indicated that SMAD4 negatively regulated the expressions of CXCL1 and CXCL8 in colorectal cancer cells.

SMAD4 regulates expression levels of CXCL1 and CXCL8 indirectly

In TGFβ signaling, ligand binding to the TGFβ receptors phosphorylates SMAD2/3 to form a heteromeric complex with SMAD4, which translocates into the nucleus and regulates transcription of target genes (17). In SW837 cells, the addition of the TGFβ1 ligand significantly decreased *CXCL1* and *CXCL8* (Supplementary Fig. S1B). The addition of TGFβ1 also induced luciferase from the SMAD-binding elements (SBE)-Luc reporter construct that contained 4 SBEs (Supplementary Fig. S1C, left), indicating that TGFβ signaling was activated via SMAD4. After the promoter region of the *CXCL1* and *CXCL8* genes (−1,320 to +77 bp and −1,353 to +89 bp from the transcription start site, respectively) was transfected into SW837 cells, we measured luciferase activity with or without TGFβ1 and found that the luciferase activities of CXCL1 and CXCL8 were not altered at all by TGFβ1 stimulation (Supplementary Fig. S1C, middle and right). Sequence analysis of the promoter/enhancer region revealed that the *CXCL1* gene contains 1 TGFβ-inhibitory element (TIE) and 1 SBE, and that the *CXCL8* gene contains 3 SBEs (Supplementary Fig. S1D). We did not observe any alterations in the promoter regions of *CXCL1* and *CXCL8* by chromatin immunoprecipitation PCR (ChIP-PCR) assay using an anti-SMAD4 antibody (Supplementary Fig. S1E), which indicated that SMAD4 does not bind to SBEs and/or TIE in the promoters of *CXCL1* and *CXCL8* gene transcription.

To identify the specific pathway by which SMAD4 regulates the expression of CXCL1 and CXCL8, we treated SW837-sh*SMAD4* cells with a series of kinase inhibitors. Based on the reduction in mRNA levels, sc-514 (Iκβ kinase 2 inhibitor) and indirubin (an inhibitor of GSK-3β and cyclin-dependent kinases) were the most prominent inhibitors of CXCL1 and CXCL8 (Supplementary Fig. S2A). Collectively, these results indicated that SMAD4 regulates the expressions of CXCL1 and CXCL8 indirectly, not by binding to their promoters.

SMAD4-negative colorectal cancer cells attract neutrophils via the CXCL8–CXCR2 axis

CXCL1 and CXCL8 are known to attract neutrophils, because neutrophils express CXCR2, the cognate receptor for CXCL1 and CXCL8 (18). Thus, we speculated that SMAD4-negative colorectal cancer cells could recruit neutrophils via the CXCL1/8-CXCR2 axis. We first isolated neutrophils from peripheral blood of healthy donors and confirmed that they were positive for CD66b and CXCR2 by flow-cytometric analysis (Fig. 3A). We also confirmed that these isolated neutrophils exhibited migratory responses to recombinant human CXCL1 and CXCL8 in a dose-dependent manner using an *in vitro* chemotaxis assay (Supplementary Fig. S2B). To simulate the biological role of neutrophils in the tumor microenvironment, neutrophils isolated from peripheral blood were added to the upper chamber, while the supernatant of colorectal cancer cells was added to the lower chamber. As expected, the migratory response of neutrophils to the supernatant of SMAD4-negative cells (SW837-sh*SMAD4* cells) was approximately twice that of the control cells (Fig. 3B). Importantly, neutrophil migration was significantly suppressed when neutralizing anti-CXCL1 or anti-CXCL8 antibody was added to the lower chamber (Fig. 3C). The suppressive effect of anti-CXCL8 antibody was more prominent compared with that of anti-CXCL1 antibody. Furthermore, treatment with SB 225002, a CXCR2 inhibitor, could completely suppress the migratory response of neutrophils (Fig. 3D). These results suggested that the SMAD4-negative colorectal cancer cells attracted neutrophils via the CXCL8–CXCR2 axis.

SMAD4-negative colorectal cancers educates neutrophils to express CXCL1 and CXCL8

We speculated that the phenotype of tumor-infiltrating neutrophils could be affected in response to the tumor microenvironment. To identify the factors secreted by neutrophils in colorectal cancer tissues, we first used a chemokine array with the neutrophils cocultured with the supernatant of colorectal cancer cells. As shown in Fig. 4A, the neutrophils cocultured with the supernatant of SMAD4-negative colorectal cancer (SW837-sh*SMAD4* cells) secreted significantly higher levels of CXCL1 and CXCL8 compared with those cocultured with the supernatant of SMAD4-positive colorectal cancer (SW837-scramble cells) (approximately 2.0-fold and 1.5-fold increases, respectively). CCL3 and CCL4 were also remarkably elevated when neutrophils were cocultured with the supernatant of SMAD4-negative colorectal cancer. We next performed an angiogenesis array and found that CXCL8 was increased most remarkably among a panel of angiogenic factors when neutrophils were cocultured with the supernatant of SMAD4-negative colorectal cancer (SW837-sh*SMAD4* cells; Fig. 4B). We also measured the mRNA levels of *CXCL1* and *CXCL8* in neutrophils by qRT-PCR. Of note, *CXCL1* and *CXCL8* were markedly increased in the neutrophils cocultured with the supernatant of SMAD4-negative colorectal cancer (SW837-sh*SMAD4* cells) compared with those cocultured with the supernatant of SMAD4-positive colorectal cancer (SW837-scramble cells; Fig. 4C). To explore the alterations of intracellular signaling pathways in neutrophils, we analyzed a phospho-kinase array and found that focal adhesion kinase and Src were significantly upregulated when neutrophils were cocultured with the supernatant of SMAD4-negative colorectal cancer (SW837-sh*SMAD4* cells; Fig. 4D). These observations support the notion that the tumor-infiltrating neutrophils can be educated by SMAD4-negative colorectal cancer. As shown in Fig. 2, CXCL1 and CXCL8 were also produced by colorectal cancer cells, and thus, we compared their expression levels in the neutrophils with those in colorectal cancer cells. The mRNA levels of CXCL1 and

Downloaded from clincancerres.aacrjournals.org on June 30, 2019. © 2019 American Association for Cancer Research.

Published OnlineFirst January 31, 2019; DOI: 10.1158/1078-0432.CCR-18-3684

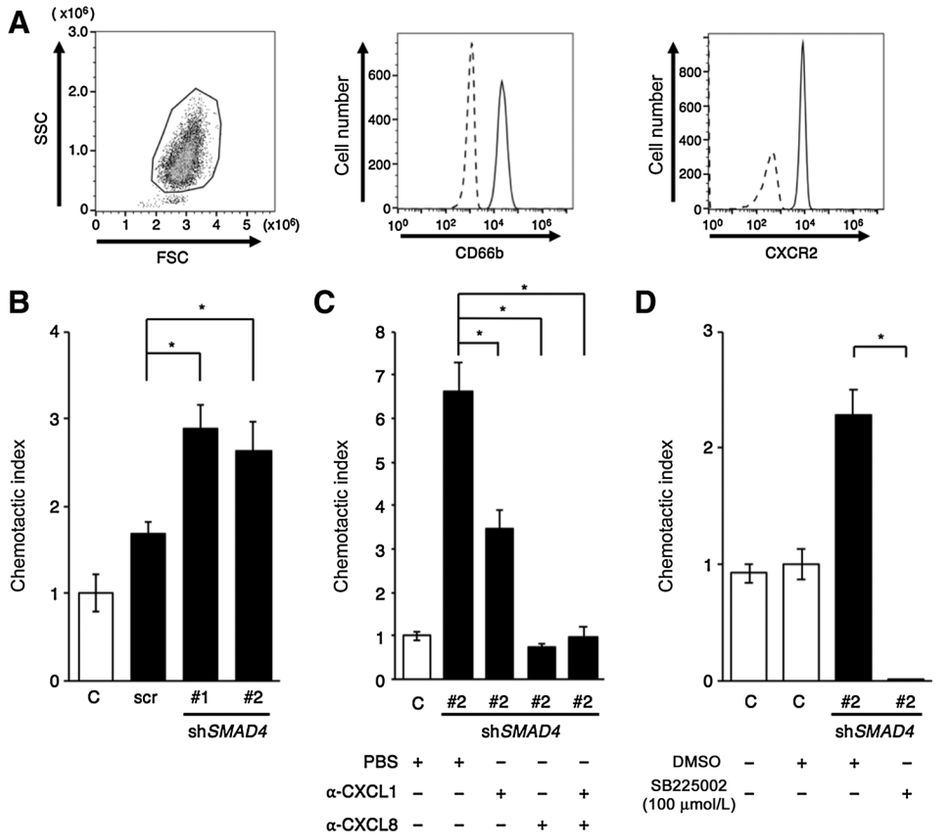

Figure 3.
Neutrophil recruitment toward SMAD4-negative colorectal cancer via the CXCL1/8–CXCR2 axis. **A,** Isolation of neutrophils from peripheral blood using the MACSxpress neutrophil isolation kit. The dotted lines show isotype control, while solid lines show anti-CD66b (middle) and anti-CXCR2 (right). **B,** Chemotactic responses of neutrophils toward the supernatant of colorectal cancer cells (SW837). C and scr indicate control medium and nonsilencing scramble. Mean; bars, ± SD. *, $P < 0.05$ by Student *t* test. **C,** Chemotactic responses of neutrophils toward the supernatant of SW837-sh*SMAD4* cells with or without neutralizing antibody for CXCL1 (20 μg/mL) and CXCL8 (10 μg/mL). Mean; bars, ± SD. *, $P < 0.05$ by Student *t* test. **D,** Chemotactic responses of neutrophils toward the supernatant of SW837-sh*SMAD4* cells with or without SB225002 (100 μmol/L). C indicates control medium (RPMI-1640). Mean; bars, ± SD. *, $P < 0.05$ by Student *t* test.

CXCL8 in the neutrophils, which were cocultured with SMAD4-negative colorectal cancer (SW837-sh*SMAD4* cells), were much higher than those in SMAD4-negative colorectal cancer cells (SW837-sh*SMAD4* cells; Fig. 4E).

TANs express CXCL1 and CXCL8

As shown in Fig. 4, we have found that neutrophils expressed CXCL1 and CXCL8 when they were cocultured with SMAD4-negative colorectal cancer cells *in vitro*. Therefore, we next examined clinical samples of primary colorectal cancer for CXCL1 and CXCL8 by IHC. IHC analysis indicated that both CXCL1 and CXCL8 were abundantly expressed in the infiltrating inflammatory cells around the peritumoral stroma of SMAD4-negative colorectal cancers compared with SMAD4-positive ones (Fig. 5A). The staining intensity of CXCL1 and CXCL8 in the tumor cells was weaker than that in the infiltrating inflammatory cells (Fig. 5A), which is in agreement with the data observed in Fig. 4E. We next characterized the cells expressing CXCL1 and CXCL8 using double immunofluorescence staining. Because anti-CD66b antibody did not work in immunofluorescence staining, we used myeloperoxidase (MPO) as a human myeloid-lineage marker. We confirmed that the distribution of MPO-positive cells was almost the same as that of $CD66b^+$ cells by IHC staining (Fig. 5A). The majority of the cells expressing CXCL1 and CXCL8 were positive for MPO (Fig. 5B), which suggested that CXCL1 and/or CXCL8 were strongly secreted by TANs in clinical colorectal cancer samples. Protumorigenic TANs are characterized by angiogenic function [by producing matrix metalloproteinases (MMP)] and immunosuppressive function (by producing ARG1 and IDO; refs. 11, 12). Consistently, we further confirmed that the majority of these MPO-positive cells were $CXCR2^+$ and expressed MMP2 and MMP9 in addition to ARG1 and IDO (Fig. 5C).

Serum CXCL8 concentration could be a novel biomarker of colorectal cancer

To explore the expression levels of CXCL1 and CXCL8 in colorectal cancer-associated TANs, we isolated the neutrophils from peripheral blood and from surgical specimens of the same patients with colorectal cancer ($n = 6$) by fluorescence-activated cell sorting with CD45, CD66b, CD14, CD15, and CD16 (Supplementary Fig. S2C). Compared with peripheral blood neutrophils, TANs derived from primary colorectal cancer expressed significantly higher levels of CXCL1 and CXCL8 (4.7-fold and 38.8-fold increase, respectively; Fig. 6A).

Serum CXCL1 and CXCL8 have been recently identified as a biomarker of melanoma, hepatocellular carcinoma (HCC), breast cancer, and prostate cancer (19–22). Therefore, we investigated whether the serum levels of CXCL1 and CXCL8 could be a biomarker for colorectal cancer progression. We measured the levels of CXCL1 and CXCL8 in serum samples from patients with colorectal cancer ($n = 125$) and healthy donors ($n = 11$) by ELISA (Supplementary Table S6). The serum CXCL8 level was significantly higher in patients with colorectal cancer than that in controls (median, 13.7 vs. 2.9 pg/mL, respectively; $P < 0.01$), whereas the serum CXCL1 level was significantly lower in colorectal cancer patients (median, 8.8 vs. 100.4 pg/mL, respectively; $P < 0.01$; Fig. 6B). We then investigated the serum CXCL8 level by the stage-based classification and found it was significantly

Downloaded from clincancerres.aacrjournals.org on June 30, 2019. © 2019 American Association for Cancer Research.

Published OnlineFirst January 31, 2019; DOI: 10.1158/1078-0432.CCR-18-3684

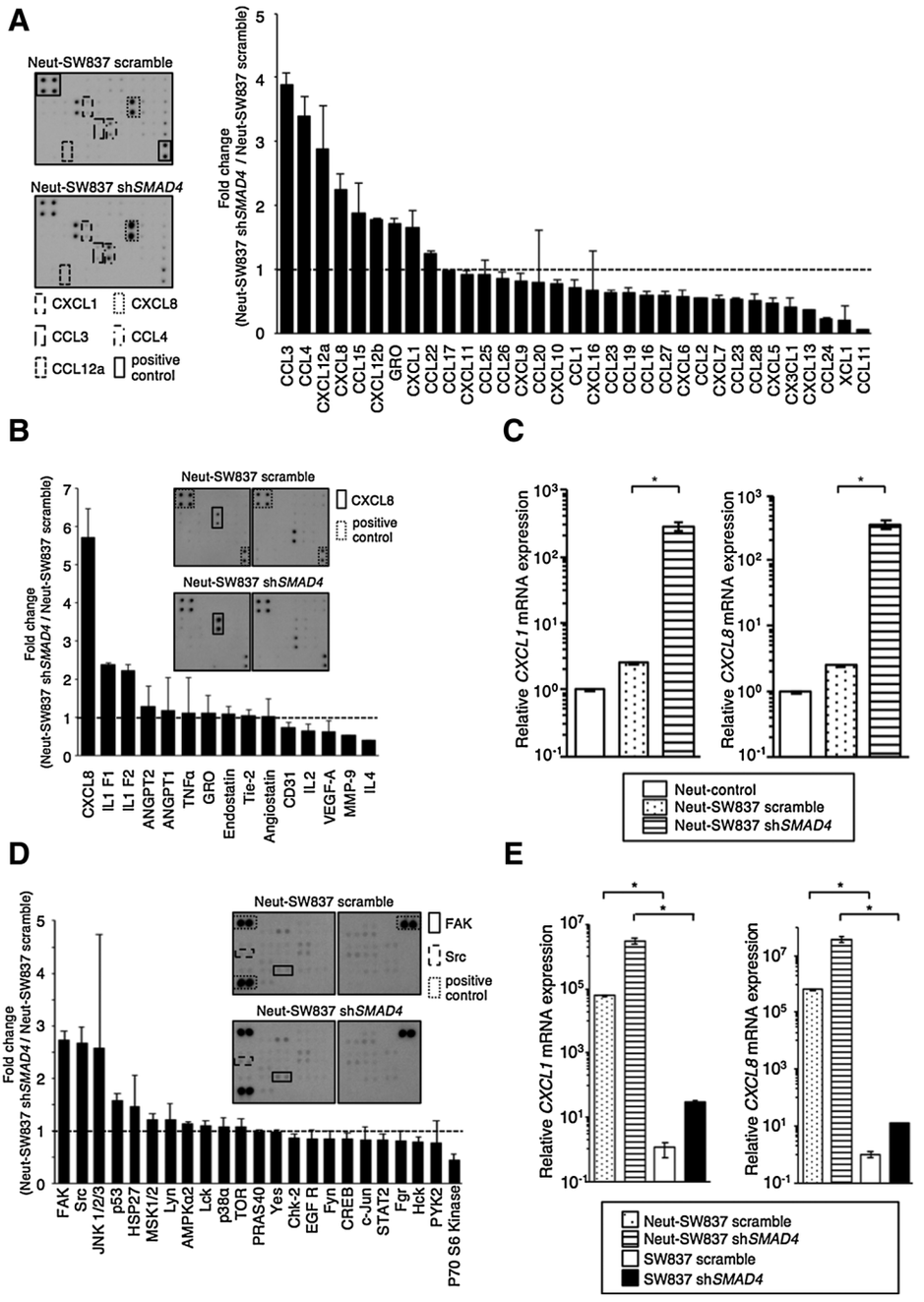

Figure 4.
Characterization of neutrophils cocultured with the supernatant of colorectal cancer cells. **A,** Chemokine array using the neutrophils cocultured with the supernatant of colorectal cancer cells (SW837-sh*SMAD4* or SW837-scramble). **B,** Angiogenesis array using the neutrophils cocultured with the supernatant of colorectal cancer cells (SW837-sh*SMAD4* or SW837-scramble). **C,** qRT-PCR analysis for *CXCL1* (left) and *CXCL8* (right). *, $P < 0.05$ by Student *t* test. **D,** Phospho-kinase array using the neutrophils cocultured with the supernatant of colorectal cancer cells (SW837-sh*SMAD4* or SW837-scramble). **E,** qRT-PCR analysis for *CXCL1* (left) and *CXCL8* (right). *, $P < 0.05$ by Student *t* test.

increased at stage II/III and then decreased at stage IV (Fig. 6C). To evaluate the clinical outcome, we analyzed the OS and RFS of the 125 patients with colorectal cancer. Statistical analysis showed that the cases with high CXCL8 level tended to exhibit a shorter OS and RFS, although not a significant difference, compared with those with low CXCL8 level ($P = 0.07$ and 0.08, respectively; Fig. 6D). In particular, the stage II/III cases with high CXCL8 level exhibited a significantly shorter OS compared with those with low CXCL8 level ($P = 0.04$; Supplementary Fig. S2D). On the other hand, there was no association between the CXCL1 concentration and prognosis. These results suggest that serum CXCL8 concentration could be a novel biomarker of colorectal cancer associated with poor prognosis.

Discussion

Accumulating evidence has emphasized the complex and multidirectional cross-talk between tumor cells and immune stromal cells, although it remains unclear how genetic alterations in tumor cells could affect stromal cells. Recently, there has been emerging interest in investigating the role of TANs in cancer. TANs can either promote or inhibit tumor progression via releasing cytokines and

Downloaded from clincancerres.aacrjournals.org on June 30, 2019. © 2019 American Association for Cancer Research.

Published OnlineFirst January 31, 2019; DOI: 10.1158/1078-0432.CCR-18-3684

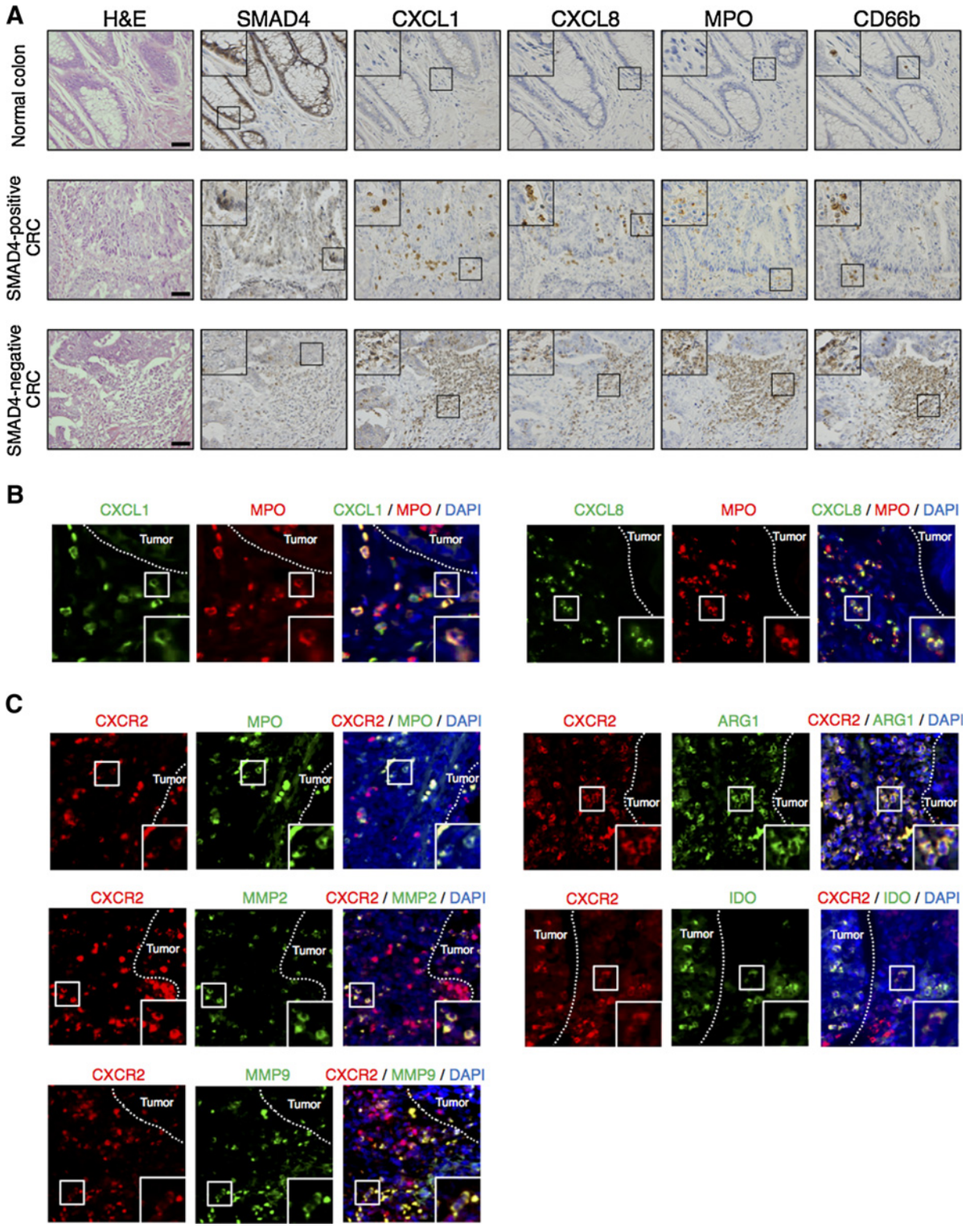

Figure 5.

Characterization of the cells expressing CXCL1 and CXCL8 in primary colorectal cancer (CRC) tissues. **A,** H&E and IHC detection of SMAD4, CXCL1, CXCL8, MPO, and CD66b. The panels show serial sections of representative normal colon (top), SMAD4-positive colorectal cancer (middle), and SMAD4-negative colorectal cancer (bottom). Scale bar, 50 μm. **B,** Simultaneous immunofluorescence staining for MPO (red) and CXCL1 or CXCL8 (green). **C,** Simultaneous immunofluorescence staining for CXCR2 (red) and MPO, MMP2, MMP9, ARG1, or IDO (green).

Downloaded from clincancerres.aacrjournals.org on June 30, 2019. © 2019 American Association for Cancer Research.

Published OnlineFirst January 31, 2019; DOI: 10.1158/1078-0432.CCR-18-3684

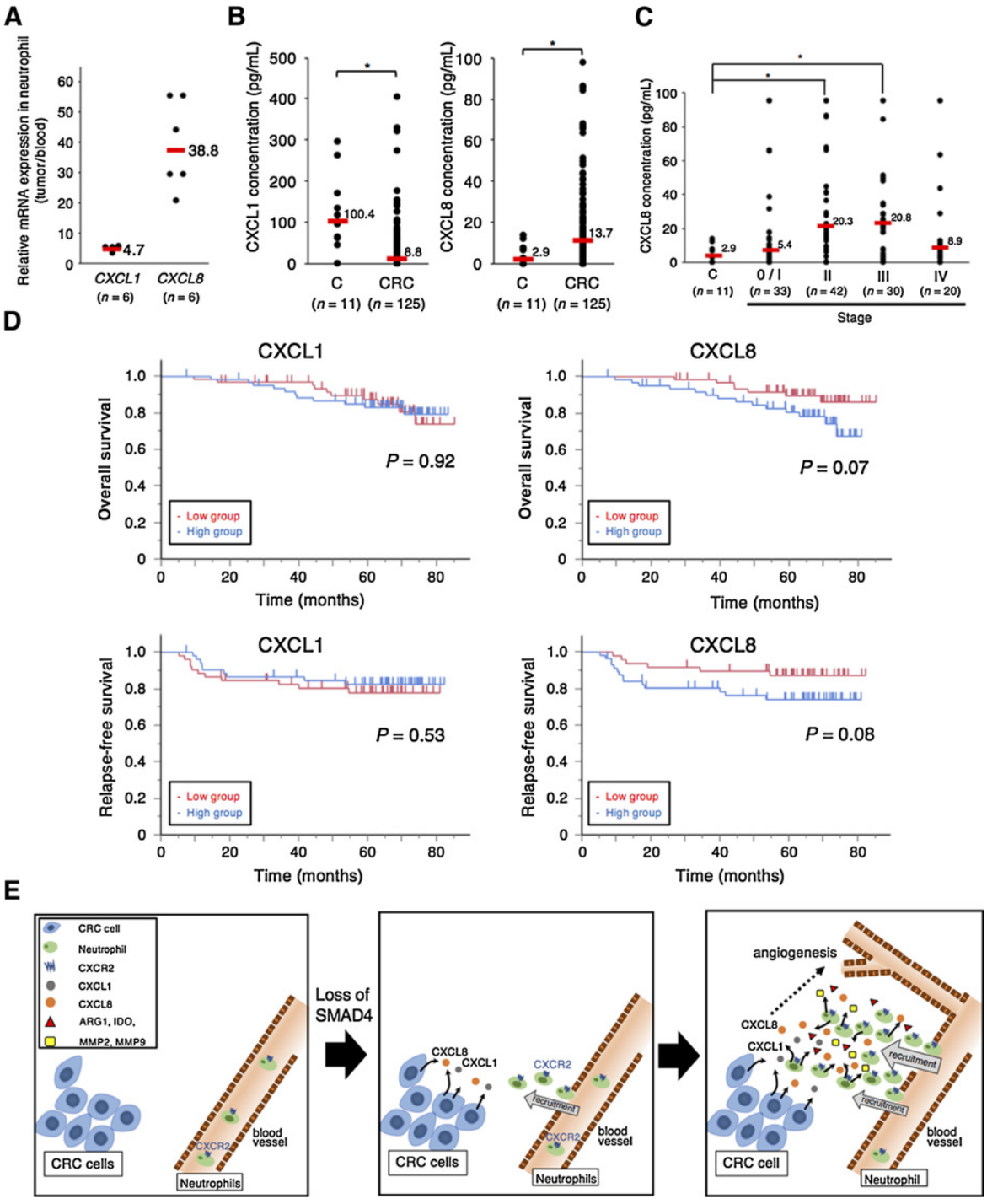

Figure 6.

Clinical significance of CXCL1 and CXCL8 in colorectal cancer (CRC). **A,** qRT-PCR analysis for *CXCL1* and *CXCL8* in neutrophils. **B,** Preoperative serum concentration of CXCL1 and CXCL8 in patients with colorectal cancer ($n = 125$) and control healthy donors ($n = 11$). *, $P < 0.05$ by Wilcoxon test. Horizontal bars show the median. **C,** Preoperative serum concentration of CXCL1 and CXCL8 in patients with colorectal cancer ($n = 125$), according to the stage-based classification. *, $P < 0.05$ by Wilcoxon test. **D,** Effect of CXCL1 (left) and CXCL8 (right) on RFS and OS in patients with colorectal cancer. Kaplan–Meier estimates. The median number of CXCL1 and CXCL8 (i.e., 8.8 and 13.7, respectively) was used as cutoff value. Kaplan–Meier estimates. *P* value was estimated by log-rank test. **E,** Schematic representation of the results. Loss of SMAD4 from colorectal cancer cells promotes expression of CXCL1 and CXCL8, followed by recruitment of $CXCR2^+$ neutrophils from the blood vessels. Thereafter, these recruited neutrophils were educated to secrete abundant CXCL1 and CXCL8, which accelerates further recruitment of $CXCR2^+$ neutrophils and promotes tumor progression by release of MMP2, MMP9, ARG1, and IDO.

Downloaded from clincancerres.aacrjournals.org on June 30, 2019. © 2019 American Association for Cancer Research.

Published OnlineFirst January 31, 2019; DOI: 10.1158/1078-0432.CCR-18-3684

chemokines, depending on the tumor microenvironment (23). In experimental models, it has been documented that neutrophils can polarize into N1 and N2 functional states: N1 neutrophils are antitumorigenic, whereas N2 neutrophils are protumorigenic (24, 25). Their surface markers, transcription regulators, and cytokine expression patterns are largely unclear. Our previous work revealed that loss of SMAD4 promoted CCL15 expression from colorectal cancer cells to recruit $CCR1^+$ myeloid cells via the CCL15–CCR1 axis, and that most $CCR1^+$ cells recruited to the primary colorectal cancer and metastatic colorectal cancer were granulocytic-MDSCs and TANs, respectively (5–7). This difference might be caused by the difficulty in distinguishing between granulocytic-MDSCs and TANs. MDSC is a term assigned to a group of myeloid cells that suppress immune responses and is a heterogeneous population at various stages of differentiation. MDSCs can differentiate into not only neutrophils and monocytes but also endothelial cells. Because MDSCs and TANs share a common set of markers and are morphologically similar, it remains unanswered whether TANs and MDSCs are separate populations or not (11, 26). In the present study, we focused on exploring the effect of SMAD4 on TAN infiltration into colorectal cancer and found that high density of marginal $CD66b^+$ neutrophils was negatively correlated with SMAD4 expression (Fig. 1A and B). Similar to our present work, a recent publication indicated that loss of Smad4 in mouse colon epithelium significantly increased the number of infiltrated neutrophils to the colon tumor compared with that in control mice (*Apc* mutant mice) by inducing several chemokines such as CCL20 and CXCL5 (8). Furthermore, we observed that SMAD4-negative colorectal cancers with high neutrophil infiltration exhibited a poorer prognosis compared with SMAD4-negative colorectal cancers with low neutrophil infiltration (Fig. 1C) and that a majority of the tumor-infiltrating neutrophils exhibited angiogenic function (by producing MMP2, MMP9, and CXCL8) and immunosuppressive function (by producing ARG1 and IDO; Fig. 5B and C), which may suggests that SMAD4-negative colorectal cancers could induce TANs to polarize into the N2 phenotype.

SMAD4 is decorated by a number of proteins that might contribute to myeloid cell infiltration and tumor progression, and the CCL15–CCR1 axis is probably only one of the players recognized to date. Therefore, we conducted a chemokine array to screen for the determinants responsible for neutrophil infiltration and found that loss of SMAD4 from colorectal cancer cells resulted in the secretion of CXCL1 and CXCL8 to recruit $CD66b^+$ neutrophils via CXCR2 (Figs. 2 and 3; Supplementary Fig. S1). In turn, the recruited neutrophils abundantly produced CXCL1 and CXCL8 (Figs. 4 and 5), which might help to further accumulate $CD66b^+$ neutrophils and result in an amplification of the cytokine/chemokine milieu within the tumor microenvironment shaped by the CXCL1/8–CXCR2 axis (Fig. 6E). Neutrophils secrete several proinflammatory, angiogenic, and immunoregulatory factors, including neutrophil elastase (27), hepatocyte growth factor (28), MMPs, and vascular endothelial growth factor (VEGF; refs. 29, 30), which can exhibit a paracrine effect on tumor cell biology. TANs have also been shown to mediate the infiltration of macrophages and regulatory T cells by secreting CCL2 and CCL17, which resulted in HCC progression (31, 32). Blocking this vicious cycle, for example, with a CXCR2 inhibitor, could be a promising treatment strategy. We also found that neutrophils abundantly produced CCL3 and CCL4 under coculture with SMAD4-negative colorectal cancer cells (Fig. 4A), which might attract mesenchymal stem cells (33) and fibroblasts (34) to result in the tumor progression of SMAD4-negative colorectal cancer.

Both CXCL1 and CXCL8 are proinflammatory mediators that function in neutrophil recruitment and activation (35, 36) and are secreted by a variety of stromal cells, including neutrophils, monocytes, fibroblasts, and endothelial cells. CXCL8 was also identified as a potent angiogenic molecule (37). CXCL8 expression has been shown to be regulated by various stimuli including inflammatory cytokines (e.g., TNFα and IL1β), chemical and environmental stresses (e.g., hypoxia and chemotherapeutic agents), reactive oxygen species, and pathogens (38, 39). The *CXCL8* gene is located on chromosome 4, and its expression can be modulated by the methylation of its promoter (40). Our study is the first to show that, in colorectal cancer cells, SMAD4 regulates the expression of CXCL1 and CXCL8 in cooperation with Iκβ kinase 2 and/or GSK-3β/cyclin-dependent kinases (Fig. 2; Supplementary Figs. S1 and S2A). A tumor-promoting role of CXCL8 and CXCL1 has been proposed in a wide variety of cancers (38, 41–43). Previous studies have reported that the CXCL1/2–S100A8/9 paracrine network between tumor cells and TANs was hyperactivated upon chemotherapy, which led to chemoresistance and lung metastasis in mouse models of breast cancer (43). Recently, Taki and colleagues reported that Snail upregulated CXCL1/2 through the NF-kB pathway and promoted ovarian cancer progression by recruiting MDSCs (44). As the elevated serum level of CXCL8 has been found to be a prognostic marker in several types of cancers (19–22), we observed that patients with colorectal cancer exhibited a significantly higher serum levels of CXCL8 compared with that of healthy donors (Fig. 6B and C), and that higher levels of CXCL8 were associated with poor prognosis (Fig. 6D). Sanmamed and colleagues recently reported serum CXCL8 concentrations were correlated with tumor burden (i.e., longest diameter) and stage in several solid tumors (45). In this study, serum CXCL8 level was increased at stage II/III and then decreased at stage IV (Fig. 6C), which may happen to reflect the tumor size of each stage. The median diameters of the primary tumor at stages II, III, and IV were 45 mm, 45 mm, and 40 mm, respectively (Supplementary Fig. S2E).

CXCR2 and its ligands (i.e., CXCL1, 2, 3, 5, 7, and 8) are responsible for recruiting neutrophils under physiologic conditions and have been implicated in TAN mobilization (46). In tumor-bearing mouse models, targeting CXCR2-meidated TAN mobilization has been shown to increase the number of tumor-infiltrating lymphocytes and potentiate anti-programmed death 1 checkpoint blockade (47–50). Recently, Nywening and colleagues reported that dual blockade of $CXCR2^+$ TANs and $CCR2^+$ TAMs disrupted myeloid cell recruitment and improved antitumor immunity in a mouse model of pancreatic ductal adenocarcinoma (51). Exposure to the tumor microenvironment may influence neutrophil plasticity, adding further complexity to understand the role of neutrophils in cancer. Further studies are required to determine the migratory mechanisms and behavior of TANs to establish the future therapies. Notably, pharmacologic inhibitors of CXCR1/2 are already used in clinical trials of inflammatory diseases (e.g., rheumatoid arthritis, asthma, and chronic obstructive pulmonary disease) as well as certain cancers (e.g., melanoma and breast cancer; ref. 39). Considering these reports and our results, blocking the CXCL1/8–CXCR2 axis could be worthwhile to inhibit progression of SMAD4-negative colorectal cancers.

Downloaded from clincancerres.aacrjournals.org on June 30, 2019. © 2019 American Association for Cancer Research.

Published OnlineFirst January 31, 2019; DOI: 10.1158/1078-0432.CCR-18-3684

Disclosure of Potential Conflicts of Interest

No potential conflicts of interest were disclosed.

Authors' Contributions

Conception and design: K. Kawada
Development of methodology: R. Ogawa, T. Yamamoto, K. Kawada
Acquisition of data (provided animals, acquired and managed patients, provided facilities, etc.): R. Ogawa, T. Yamamoto, H. Hirai, K. Hanada, Y. Kiyasu, G. Nishikawa
Analysis and interpretation of data (e.g., statistical analysis, biostatistics, computational analysis): R. Ogawa, T. Yamamoto, K. Kawada
Writing, review, and/or revision of the manuscript: R. Ogawa, T. Yamamoto, H. Hirai, R. Mizuno, Y. Itatani, K. Kawada
Administrative, technical, or material support (i.e., reporting or organizing data, constructing databases): Y. Kiyasu, G. Nishikawa, S. Inamoto, Y. Itatani
Study supervision: Y. Sakai

Acknowledgments

The authors thank Yoshikage Inoue, Riki Ganeko, and Atsushi Yamada for providing fruitful comments regarding statistical analyses. This work was supported by grants from the Ministry of Education, Culture, Sports, Science and Technology of Japan, from Project Mirai Cancer Research, and from The NOVARTIS Foundation (Japan) for the Promotion of Science (to K. Kawada).

The costs of publication of this article were defrayed in part by the payment of page charges. This article must therefore be hereby marked *advertisement* in accordance with 18 U.S.C. Section 1734 solely to indicate this fact.

Received November 9, 2018; revised January 4, 2019; accepted January 28, 2019; published first January 31, 2019.

References

1. Roth AD, Delorenzi M, Tejpar S, Yan P, Klingbiel D, Fiocca R, et al. Integrated analysis of molecular and clinical prognostic factors in stage II/III colon cancer. J Natl Cancer Inst 2012;104:1635–46.
2. Voorneveld PW, Jacobs RJ, Kodach LL, Hardwick JC. A meta-analysis of SMAD4 immunohistochemistry as a prognostic marker in colorectal cancer. Transl Oncol 2015;8:18–24.
3. Takaku K, Oshima M, Miyoshi H, Matsui M, Seldin MF, Taketo MM. Intestinal tumorigenesis in compound mutant mice of both Dpc4 (Smad4) and Apc genes. Cell 1998;92:645–56.
4. Kitamura T, Kometani K, Hashida H, Matsunaga A, Miyoshi H, Hosogi H, et al. SMAD4-deficient intestinal tumors recruit CCR1+ myeloid cells that promote invasion. Nat Genet 2007;39:467–75.
5. Itatani Y, Kawada K, Fujishita T, Kakizaki F, Hirai H, Matsumoto T, et al. Loss of SMAD4 from colorectal cancer cells promotes CCL15 expression to recruit CCR1+ myeloid cells and facilitate liver metastasis. Gastroenterology 2013;145:1064–75.
6. Inamoto S, Itatani Y, Yamamoto T, Minamiguchi S, Hirai H, Iwamoto M, et al. Loss of SMAD4 promotes colorectal cancer progression by accumulation of myeloid-derived suppressor cells through the CCL15-CCR1 chemokine axis. Clin Cancer Res 2016;22:492–501.
7. Yamamoto T, Kawada K, Itatani Y, Inamoto S, Okamura R, Iwamoto M, et al. Loss of SMAD4 promotes lung metastasis of colorectal cancer by accumulation of CCR1+ tumor-associated neutrophils through CCL15-CCR1 Axis. Clin Cancer Res 2017;23:833–44.
8. Means AL, Freeman TJ, Zhu J, Woodbury LG, Marincola-Smith P, Wu C, et al. Epithelial Smad4 deletion up-regulates inflammation and promotes inflammation-associated cancer. Cell Mol Gastroenterol Hepatol 2018;6:257–76.
9. Pages F, Mlecnik B, Marliot F, Bindea G, Ou FS, Bifulco C, et al. International validation of the consensus Immunoscore for the classification of colon cancer: a prognostic and accuracy study. Lancet 2018;391:2128–39.
10. Kitamura T, Qian BZ, Pollard JW. Immune cell promotion of metastasis. Nat Rev Immunol 2015;15:73–86.
11. Coffelt SB, Wellenstein MD, de Visser KE. Neutrophils in cancer: neutral no more. Nat Rev Cancer 2016;16:431–46.
12. Engblom C, Pfirschke C, Pittet MJ. The role of myeloid cells in cancer therapies. Nat Rev Cancer 2016;16:447–62.
13. Templeton AJ, McNamara MG, Seruga B, Vera-Badillo FE, Aneja P, Ocana A, et al. Prognostic role of neutrophil-to-lymphocyte ratio in solid tumors: a systematic review and meta-analysis. J Natl Cancer Inst 2014;106:dju124.
14. Fridlender ZG, Albelda SM. Tumor-associated neutrophils: friend or foe? Carcinogenesis 2012;33:949–55.
15. Granot Z, Jablonska J. Distinct functions of neutrophil in cancer and its regulation. Mediators Inflamm 2015;2015:701067.
16. Sagiv JY, Michaeli J, Assi S, Mishalian I, Kisos H, Levy L, et al. Phenotypic diversity and plasticity in circulating neutrophil subpopulations in cancer. Cell Rep 2015;10:562–73.
17. Massague J, Seoane J, Wotton D. Smad transcription factors. Genes Dev 2005;19:2783–810.
18. Lazennec G, Richmond A. Chemokines and chemokine receptors: new insights into cancer-related inflammation. Trends Mol Med 2010;16:133–44.
19. Ugurel S, Rappl G, Tilgen W, Reinhold U. Increased serum concentration of angiogenic factors in malignant melanoma patients correlates with tumor progression and survival. J Clin Oncol 2001;19:577–83.
20. Ren Y, Poon RT, Tsui HT, Chen WH, Li Z, Lau C, et al. Interleukin-8 serum levels in patients with hepatocellular carcinoma: correlations with clinicopathological features and prognosis. Clin Cancer Res 2003;9:5996–6001.
21. Benoy IH, Salgado R, Van Dam P, Geboers K, Van Marck E, Scharpe S, et al. Increased serum interleukin-8 in patients with early and metastatic breast cancer correlates with early dissemination and survival. Clin Cancer Res 2004;10:7157–62.
22. Veltri RW, Miller MC, Zhao G, Ng A, Marley GM, Wright GL Jr, et al. Interleukin-8 serum levels in patients with benign prostatic hyperplasia and prostate cancer. Urology 1999;53:139–47.
23. Tecchio C, Scapini P, Pizzolo G, Cassatella MA. On the cytokines produced by human neutrophils in tumors. Semin Cancer Biol 2013;23:159–70.
24. Fridlender ZG, Sun J, Kim S, Kapoor V, Cheng G, Ling L, et al. Polarization of tumor-associated neutrophil phenotype by TGF-beta: "N1" versus "N2" TAN. Cancer Cell 2009;16:183–94.
25. Mantovani A, Cassatella MA, Costantini C, Jaillon S. Neutrophils in the activation and regulation of innate and adaptive immunity. Nat Rev Immunol 2011;11:519–31.
26. Bronte V, Brandau S, Chen SH, Colombo MP, Frey AB, Greten TF, et al. Recommendations for myeloid-derived suppressor cell nomenclature and characterization standards. Nat Commun 2016;7:12150.
27. Houghton AM, Rzymkiewicz DM, Ji H, Gregory AD, Egea EE, Metz HE, et al. Neutrophil elastase-mediated degradation of IRS-1 accelerates lung tumor growth. Nat Med 2010;16:219–23.
28. Wislez M, Rabbe N, Marchal J, Milleron B, Crestani B, Mayaud C, et al. Hepatocyte growth factor production by neutrophils infiltrating bronchioloalveolar subtype pulmonary adenocarcinoma: role in tumor progression and death. Cancer Res 2003;63:1405–12.
29. Kuang DM, Zhao Q, Wu Y, Peng C, Wang J, Xu Z, et al. Peritumoral neutrophils link inflammatory response to disease progression by fostering angiogenesis in hepatocellular carcinoma. J Hepatol 2011;54:948–55.
30. Liang J, Piao Y, Holmes L, Fuller GN, Henry V, Tiao N, et al. Neutrophils promote the malignant glioma phenotype through S100A4. Clin Cancer Res 2014;20:187–98.
31. Mishalian I, Bayuh R, Eruslanov E, Michaeli J, Levy L, Zolotarov L, et al. Neutrophils recruit regulatory T-cells into tumors via secretion of CCL17–a new mechanism of impaired antitumor immunity. Int J Cancer 2014;135:1178–86.
32. Zhou SL, Zhou ZJ, Hu ZQ, Huang XW, Wang Z, Chen EB, et al. Tumor-associated neutrophils recruit macrophages and T-regulatory cells to promote progression of hepatocellular carcinoma and resistance to sorafenib. Gastroenterology 2016;150:1646–58.
33. Sordi V, Malosio ML, Marchesi F, Mercalli A, Melzi R, Giordano T, et al. Bone marrow mesenchymal stem cells express a restricted set of functionally active chemokine receptors capable of promoting migration to pancreatic islets. Blood 2005;106:419–27.

Downloaded from clincancerres.aacrjournals.org on June 30, 2019. © 2019 American Association for Cancer Research.

Published OnlineFirst January 31, 2019; DOI: 10.1158/1078-0432.CCR-18-3684

34. Sasaki S, Baba T, Shinagawa K, Matsushima K, Mukaida N. Crucial involvement of the CCL3-CCR5 axis-mediated fibroblast accumulation in colitis-associated carcinogenesis in mice. Int J Cancer 2014;135: 1297–306.
35. Schroder JM, Persoon NL, Christophers E. Lipopolysaccharide-stimulated human monocytes secrete, apart from neutrophil-activating peptide 1/ interleukin 8, a second neutrophil-activating protein. NH2-terminal amino acid sequence identity with melanoma growth stimulatory activity. J Exp Med 1990;171:1091–100.
36. Moser B, Clark-Lewis I, Zwahlen R, Baggiolini M. Neutrophil-activating properties of the melanoma growth-stimulatory activity. J Exp Med 1990; 171:1797–802.
37. Koch AE, Polverini PJ, Kunkel SL, Harlow LA, DiPietro LA, Elner VM, et al. Interleukin-8 as a macrophage-derived mediator of angiogenesis. Science 1992;258:1798–801.
38. Waugh DJ, Wilson C. The interleukin-8 pathway in cancer. Clin Cancer Res 2008;14:6735–41.
39. Ha H, Debnath B, Neamati N. Role of the CXCL8-CXCR1/2 axis in cancer and inflammatory diseases. Theranostics 2017;7:1543–88.
40. De Larco JE, Wuertz BR, Yee D, Rickert BL, Furcht LT. Atypical methylation of the interleukin-8 gene correlates strongly with the metastatic potential of breast carcinoma cells. Proc Natl Acad Sci U S A 2003;100:13988–93.
41. Mizukami Y, Jo WS, Duerr EM, Gala M, Li J, Zhang X, et al. Induction of interleukin-8 preserves the angiogenic response in HIF-1α-deficient colon cancer cells. Nat Med 2005;11:992–7.
42. Asfaha S, Dubeykovskiy AN, Tomita H, Yang X, Stokes S, Shibata W, et al. Mice that express human interleukin-8 have increased mobilization of immature myeloid cells, which exacerbates inflammation and accelerates colon carcinogenesis. Gastroenterology 2013;144: 155–66.
43. Acharyya S, Oskarsson T, Vanharanta S, Malladi S, Kim J, Morris PG, et al. A CXCL1 paracrine network links cancer chemoresistance and metastasis. Cell 2012;150:165–78.
44. Taki M, Abiko K, Baba T, Hamanishi J, Yamaguchi K, Murakami R, et al. Snail promotes ovarian cancer progression by recruiting myeloid-derived suppressor cells via CXCR2 ligand upregulation. Nat Commun 2018;9:1685.
45. Sanmamed MF, Carranza-Rua O, Alfaro C, Onate C, Martin-Algarra S, Perez G, et al. Serum interleukin-8 reflects tumor burden and treatment response across malignancies of multiple tissue origins. Clin Cancer Res 2014;20: 5697–707.
46. Eash KJ, Greenbaum AM, Gopalan PK, Link DC. CXCR2 and CXCR4 antagonistically regulate neutrophil trafficking from murine bone marrow. J Clin Invest 2010;120:2423–31.
47. Highfill SL, Cui Y, Giles AJ, Smith JP, Zhang H, Morse E, et al. Disruption of CXCR2-mediated MDSC tumor trafficking enhances anti-PD1 efficacy. Sci Transl Med 2014;6:237ra67.
48. Steele CW, Karim SA, Leach JDG, Bailey P, Upstill-Goddard R, Rishi L, et al. CXCR2 inhibition profoundly suppresses metastases and augments immunotherapy in pancreatic ductal adenocarcinoma. Cancer Cell 2016;29: 832–45.
49. Jamieson T, Clarke M, Steele CW, Samuel MS, Neumann J, Jung A, et al. Inhibition of CXCR2 profoundly suppresses inflammation-driven and spontaneous tumorigenesis. J Clin Invest 2012;122:3127–44.
50. Katoh H, Wang D, Daikoku T, Sun H, Dey SK, Dubois RN. CXCR2-expressing myeloid-derived suppressor cells are essential to promote colitis-associated tumorigenesis. Cancer Cell 2013;24:631–44.
51. Nywening TM, Belt BA, Cullinan DR, Panni RZ, Han BJ, Sanford DE, et al. Targeting both tumour-associated $CXCR2^+$ neutrophils and $CCR2^+$ macrophages disrupts myeloid recruitment and improves chemotherapeutic responses in pancreatic ductal adenocarcinoma. Gut 2018;67:1112–23.

Downloaded from clincancerres.aacrjournals.org on June 30, 2019. © 2019 American Association for Cancer Research.

Published OnlineFirst January 31, 2019; DOI: 10.1158/1078-0432.CCR-18-3684

AACR American Association for Cancer Research

Clinical Cancer Research

Loss of SMAD4 Promotes Colorectal Cancer Progression by Recruiting Tumor-Associated Neutrophils via the CXCL1/8–CXCR2 Axis

Ryotaro Ogawa, Takamasa Yamamoto, Hideyo Hirai, et al.

Clin Cancer Res 2019;25:2887-2899. Published OnlineFirst January 31, 2019.

Updated version	Access the most recent version of this article at: doi:10.1158/1078-0432.CCR-18-3684
Supplementary Material	Access the most recent supplemental material at: http://clincancerres.aacrjournals.org/content/suppl/2019/02/08/1078-0432.CCR-18-3684.DC1

Cited articles	This article cites 51 articles, 17 of which you can access for free at: http://clincancerres.aacrjournals.org/content/25/9/2887.full#ref-list-1

E-mail alerts	Sign up to receive free email-alerts related to this article or journal.
Reprints and Subscriptions	To order reprints of this article or to subscribe to the journal, contact the AACR Publications Department at pubs@aacr.org.
Permissions	To request permission to re-use all or part of this article, use this link http://clincancerres.aacrjournals.org/content/25/9/2887. Click on "Request Permissions" which will take you to the Copyright Clearance Center's (CCC) Rightslink site.

Downloaded from clincancerres.aacrjournals.org on June 30, 2019. © 2019 American Association for Cancer Research.

Supplementary figure legends

Supplementary Figure 1. A, Chemokine array using the SW837 cells engineered with stable *SMAD4*-knockdown (SW837-sh*SMAD4* #2) and scramble control. Comparison of a panel of chemokines was shown. B, qRT-PCR analysis using SW837 cells with or without 10ng/mL TGF-β1 for 6 h. NT indicate nontreatment as control. *$P < 0.05$ by Student's *t*-test. C, Luciferase reporter assay showing activities of SBE4-Luc, *CXCL1*-Luc and *CXCL8*-Luc. *$P < 0.05$ by Student's *t*-test. D, Schematic representation of the *CXCL1* or *CXCL*8 gene. The sequence of this region was obtained by sequencing genomic DNA of SW837, and matches with that of database obtained from UCSC genome browser. Transcription start site (black arrow) was confirmed by 5' rapid amplification of cDNA end. E, ChIP-PCR analysis for enrichment of SBE or TIE in the promotor region of CXCL1 or CXCL8.

Supplementary Figure 2. A, Screening with a series of kinase inhibitors treated for 24 hours. qRT-PCR analysis for *CXCL1* (top) and *CXCL8* (bottom). B, Chemotactic responses of neutrophils toward the human recombinant CXCL1 and CXCL8. Mean; *bars*, ± SD. *$P < 0.05$ by Student's *t*-test. C, Neutrophils were isolated from peripheral blood and from CRC specimens of the same patients (n = 6) by FACS with CD45, CD66b, CD14, CD15, and CD16.

Supplementary Figure 1

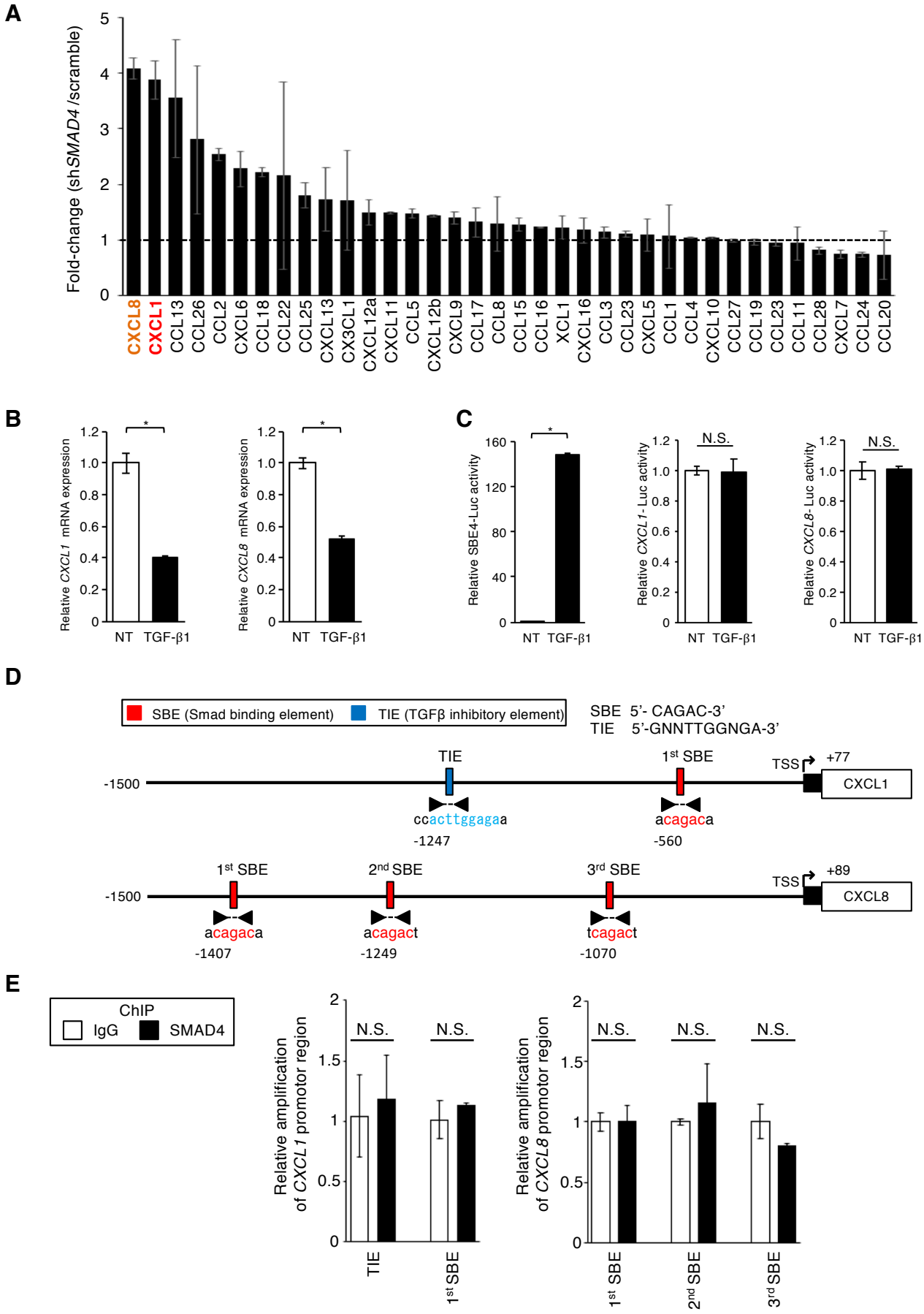

Supplementary Figure 2

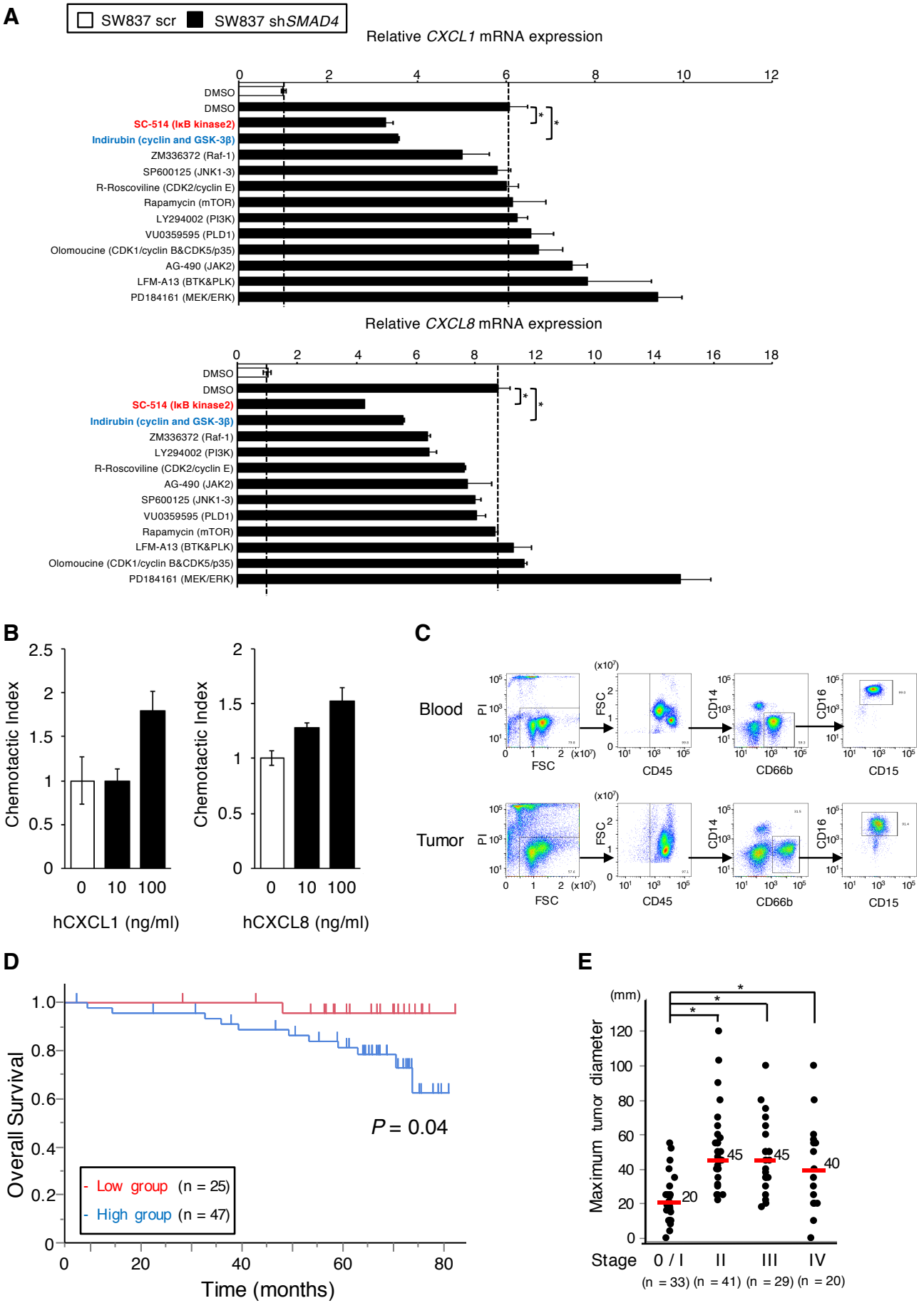

Supplementary Table S1. List of antibodies used for IHC, IF and western blotting.

Antibody	Host	Company	Dilution(WB)	Dilution(IHC/IF)
anti-SMAD4	mouse	Santa Cruz	1:1000	1:100
anti-SMAD1	Rabbit	Cell Signaling	1:1000	
anti-SMAD2/3	Rabbit	Cell Signaling	1:1000	
anti-SMAD5	Rabbit	Cell Signaling	1:1000	
anti-ACTB	Mouse	Sigma-Aldrich	1:8000	
anti-CD66b	Mouse	Biolegend		1:50
anti-MPO	Mouse	Leica		ready to use
anti-CXCR2	Rabbit	Abcam		1:100
anti-CXCL1	Goat	Santa Cruz		1:200
anti-CXCL8(IF)	Goat	R&D		1:40
anti-CXCL8(IHC)	Mouse	Abcam		1:100
anti-ARG1	Mouse	R&D		1:50
anti-IDO	Mouse	Abcam		1:100
anti-MMP2	Mouse	Abcam		1:100
anti-MMP9	Mouse	Santa Cruz		1:100

Supplementary Table S2. Kinase Inhibitors

Substance	Target of inhibition	IC50	Concentration used	Company
SC-514	IκB kinase2	IKK2 : 3-12μM	12μM	Cayman chemical
Indirubin	cyclin	CDK1/5 : 10μM	2.5μM	Cayman chemical
	GSK-3β	GSK3β : 2.5μM		
ZM336372	Raf-1	70nM	70nM	Cayman chemical
SP 600125	JNK1-3	JNK1-3 : 0.11μM	0.2μM	Cayman chemical
R-Roscoviline	CDK2/cycline E	CDK2 : 0.1μM	0.1μM	Cayman chemical
Rapamycin	mTOR	5pM	5pM	Cayman chemical
LY294002	PI3K	1.4μM	2μM	Cayman chemical
VU0359595	PLD1	3.7nM	3.7nM	Cayman chemical
Olomoucine	CDK1/cyclinB	CDK1/cyclin B : 2μM	3μM	Enzo life science
	CDK5/p35	CDK5/p35 : 3μM		
AG-490	JAK2	5μM	10uM	Cayman chemical
LFM-A13	BTK	BTK : 2.5μM	10μM	Cayman chemical
	Plk	Plk : 10μM		
PD 184161	MEK/ERK	MEK1/2 : 10-100nM	10μM	Cayman chemical

IC50, median inhibitory concentration

I

Supplementary Table S3. List of primers for ChIP assay

Region	Forward (‘5- ‘3)	Reverse (‘5- ‘3)
CXCL1 TIE	GTCTCAGAGAGCTCTGAATC	CAGTCATTTAACCTGGTAGC
CXCL1 1st SBE	CTGGAATCTGACATAATGGAC	GCTGGAGCTATATTATCCTC
CXCL8 1st SBE	TCAAGTCTTAGGTTGGTTGG	CGACAGAGCAGTGAATTTGC
CXCL8 2nd SBE	CAGTGTGGGCAAATTCACTG	AGCACCAAGGAAGGGTTCTT
CXCL8 3rd SBE	GGACACTAGGACATAAAGCC	CATCTGGGTTCCAACTCTGG

Supplementary Table S4. List of antibodies used for Flow cytometry

Antibody	Host	Clone	Company
PE anti-human CD14	Mouse	M5E2	BD
FITC anti-human CD15	Mouse	HI98	BD
APCH7 anti-human CD16	Mouse	3G8	BD
PEcy7 anti-human CD45	Mouse	HI30	BD
V450 anti-human CD66b	Mouse	G10F5	BD
FITC- anti-human CD66b	Mouse	G10F5	Biolegend
APC-anti human CXCR2	Mouse	6C6	BD

Supplementary Table S5. Patient and tumor characteristics (n = 99)

Characteristics	No. of Patients
Age, years	
Mean ± SD	67.4 ± 11.2
Sex	
Male	64
Female	35
Location	
Colon	75
Rectum	24
Histology	
tub1 / tub2	91
others	8
T factor	
Tis / T1 / T2	24
T3 / T4	75
N factor	
Negative	68
Positive	31
UICC-TNM Stage	
0, I	19
II ,III	80
CEA, ng/mL	
< 5	60
≥ 5	39
CA19-9, U/mL	
< 37	88
≥ 37	11
SMAD4	
Negative	56
Positive	43

Supplementary Table S6. Tumor characteristics. Preoperative serum samples from another cohort of 125 patients.

Characteristics	No. of Patients
Age, years	
Mean ± SD	66.0 ± 12.5
Sex	
Male	65
Female	60
Location	
Colon	88
Rectum	37
Histology	
tub1 / tub2	109
others	16
T factor	
Tis / T1 / T2	85
T3 / T4	40
N factor	
Negative	84
Positive	41
M factor	
Negative	105
Positive	20
UICC-TNM Stage	
0, I, II	75
III, IV	50
CEA, ng/mL	
< 5	80
≥ 5	45
CA19-9, U/mL	
< 37	104
≥ 37	21
CXCL1	
≤ 8.8	63
> 8.8	62
CXCL8	
≤ 13.7	63
> 13.7	62